J. Phycol. **45,** 938–952 (2009)

DOI: 10.1111/j.1529-8817.2009.00712.x

GYMNODINIUM COROLLARIUM SP. NOV. (DINOPHYCEAE)—A NEW COLD-WATER DINOFLAGELLATE RESPONSIBLE FOR CYST SEDIMENTATION EVENTS IN THE BALTIC SEA[1]

Annica M. Sundström[2]

Department of Systems Ecology, Stockholm University, SE-106 91 Stockholm, Sweden

Anke Kremp

Finnish Environment Institute, Mechelininkatu 34A, 00251 Helsinki, Finland
Tvärminne Zoological Station, University of Helsinki, J.A. Palmenintie 260, FI-10900 Hanko, Finland

Niels Daugbjerg, Øjvind Moestrup, Marianne Ellegaard

Phycology Laboratory, Department of Biology, University of Copenhagen, Øster Farimagsgade 2D, DK-1353 Copenhagen K, Denmark

Regina Hansen

Leibniz Institute for Baltic Sea Research Warnemünde, Seestraße 15, D-18119 Rostock, Germany

and Susanna Hajdu

Department of Systems Ecology, Stockholm University, SE-106 91 Stockholm, Sweden

A naked dinoflagellate with a unique arrangement of chloroplasts in the center of the cell was isolated from the northern Baltic proper during a spring dinoflagellate bloom (March 2005). Morphological, ultrastructural, and molecular analyses revealed this dinoflagellate to be undescribed and belonging to the genus *Gymnodinium* F. Stein. *Gymnodinium corollarium* A. M. Sundström, Kremp et Daugbjerg sp. nov. possesses features typical of *Gymnodinium* sensu stricto, such as nuclear chambers and an apical groove running in a counterclockwise direction around the apex. Phylogenetic analyses based on partial nuclear-encoded LSU rDNA sequences place the species in close proximity to *G. aureolum*, but significant genetic distance, together with distinct morphological features, such as the position of chloroplasts, clearly justifies separation from this species. Temperature and salinity experiments revealed a preference of *G. corollarium* for low salinities and temperatures, confirming it to be a cold-water species well adapted to the brackish water conditions in the Baltic Sea. At nitrogen-deplete conditions, *G. corollarium* cultures produced small, slightly oval cysts resembling a previously unidentified cyst type commonly found in sediment trap samples collected from the northern and central open Baltic Sea. Based on LSU rDNA comparison, these cysts were assigned to *G. corollarium*. The cysts have been observed in many parts of the Baltic Sea, indicating the ecologic versatility of the species and its importance for the Baltic ecosystem.

Key index words: **Baltic Sea; dinoflagellate cysts; *Gymnodinium*; LSU rDNA; spring bloom; taxonomy**

***Abbreviations:* BA, Bayesian analysis; CTAB, 2X hexadecyltrimethyl-ammonium bromide; GTR, general time reversible; MP, maximum parsimony; NJ, neighbor joining; TMA, tetramethylammonium chloride**

In the Baltic Sea, dinoflagellates are a common component of the spring phytoplankton community (Hobro 1979, Kononen and Niemi 1984, Wasmund et al. 1998, Hajdu 2002). Together with diatoms, they account for most of the annual new production. Although dominance patterns vary regionally and interannually, a general trend of increasing dinoflagellate abundance together with lower abundance of co-occurring diatoms has been observed over the last decades (Wasmund and Uhlig 2003). Since the early 1980s, blooms of cold-water dinoflagellates have become a recurrent phenomenon, particularly in the central and northern parts of the Baltic Sea (Lignell et al. 1993, Jaanus et al. 2006).

The taxonomic affiliations of the dinoflagellates causing these mass occurrences have long been unclear (reviewed in Kremp et al. 2005). The reason is that these blooms are constituted by medium-sized, apparently unarmored cells, which have

[1]Received 17 September 2008. Accepted 25 February 2009.
[2]Author for correspondence: e-mail annica@ecology.su.se.

hampered identification to species level in both live and fixed samples. The blooms have been attributed to different taxa, such as *Glenodinium* Ehrenb. (Hobro 1979, Müller-Haeckel 1985, Kuosa 1986, Niemi 1986), *Gymnodinium* (Niemi 1975, Autio et al. 1990, Thomsen 1992, Lignell et al. 1993), and *Peridinium hangoei* J. Schiller (Heiskanen 1993). After the redescription and transfer of the latter to *Scrippsiella hangoei* (J. Schiller) J. Larsen, this species was generally considered responsible for the dinoflagellate spring blooms, particularly in the coastal central and northern Baltic Sea (Olli et al. 1998, Kremp and Heiskanen 1999, Höglander et al. 2004, Jaanus et al. 2006). It was suggested that due to the delicate nature of its plates, the species might have been confused with and identified as unarmored taxa.

Morphological and molecular reinvestigation of cultured isolates of spring dinoflagellates revealed, however, that several species of similar shape and size co-occur in the blooms previously attributed to *S. hangoei*. Isolates from the southwest coast of Finland were identified as *Woloszynskia halophila* (Biecheler) Elbr. et Kremp, a lightly armored species with delicate platelets, which forms characteristic short-spined resting cysts (Kremp et al. 2005). *W. halophila* is recognized as the main bloom former in the Gulf of Finland (A. Sundström, personal observation), whereas *S. hangoei* presumably co-occurs in low abundances and appears to be associated with sea ice (Rintala et al. 2007).

In spring 2005, a medium-sized, single-celled dinoflagellate characterized by chloroplasts located in the central portion of the cell was isolated from a field sample collected during spring in the northern Baltic proper. Molecular, morphological, and ultrastructural analyses of cultures established from the isolates revealed morphological features typical for the genus *Gymnodinium* (as redefined by Daugbjerg et al. 2000) and indicated this dinoflagellate to be an undescribed species, *G. corollarium* sp. nov., which we describe here.

The small oval cysts formed by this species in culture resemble a hitherto unidentified cyst type found in sedimentation traps from the open Baltic proper in late spring (R. Hansen, personal observation, S. Hajdu and H. Höglander, personal communication). To examine whether the cysts from field samples are produced by *G. corollarium*, we performed DNA analyses of field material and compared LSU rDNA data to respective sequences of the *G. corollarium* isolate characterized here.

MATERIALS AND METHODS

Cultures. The clonal isolate of *G. corollarium*, GCTV-B4, was obtained from a net sample (>10 μm) collected in March 2005 from the offshore station BY29 (58°53′ N, 20°19′ E) south of the Åland Islands in the northern Baltic proper (Fig. 1). Replicate cultures established from a single cell isolate are maintained at the Tvärminne Zoological Station at 4°C, ~50 μmol photons · m^{-2} · s^{-1} and a 14:10 light:dark (L:D) cycle in f/2-Si medium (Guillard and Ryther 1962) made from local seawater (salinity of 6–7). Cyst formation was triggered by growing cultures of GCTV-B4 at reduced (f/8) nitrate concentrations. Molecular, morphological, and pigment analyses were performed at the University of Copenhagen, where culture conditions differed somewhat (salinity 7, 4°C, 35 μmol photons · m^{-2} · s^{-1} and a 16:8 L:D) from the maintenance conditions at Tvärminne. Salinities are given in practical salinity units (psu) throughout this paper.

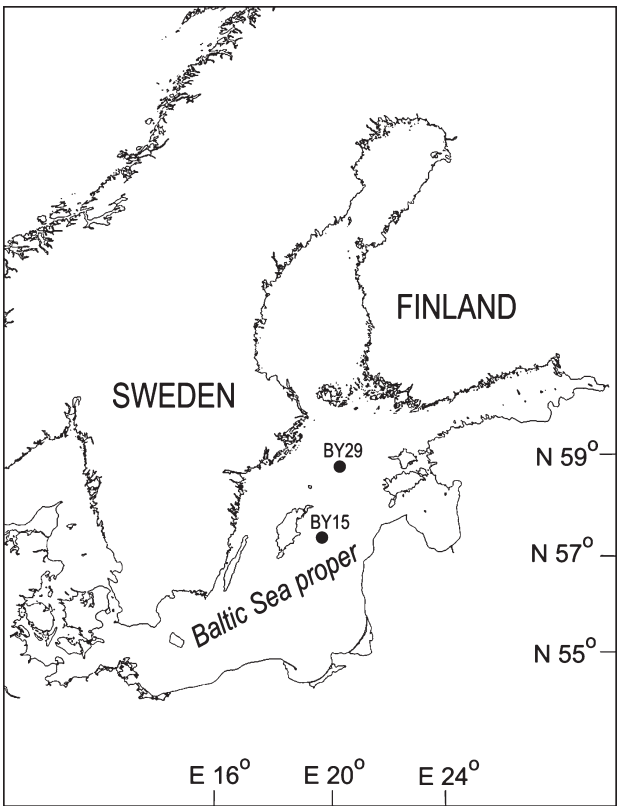

FIG. 1. Map of the Baltic Sea. BY29 = Type locality of *Gymnodinium corollarium*. BY15 = Sampling station of sediment trap cysts produced by *G. corollarium*.

LM. Vegetative cells and live cysts were observed with an Olympus Provis AX70 microscope (Olympus, Tokyo, Japan) fitted with a Zeiss AxioCam camera system (Zeiss, Jena, Germany), using differential interference contrast (DIC) and epifluorescence settings.

SEM. For SEM, flagellate cells of an exponentially growing culture and cysts from a stationary phase culture of GCTV-B4 were fixed for 30 min in 2% OsO_4 (1:1 of culture and 4% OsO_4) at room temperature. After fixation, the cells were filtered onto 5.0 μm TMTP Millipore Isopore™ Membrane Filters (Millipore, Billerica, MA, USA) and washed in distilled water for 1.5 h followed by a dehydration series of increasing ethanol concentrations (30, 50, 70, 96, and 99%). The cells were left in the respective concentration for 20 min and an additional 30 min in the final dehydration concentration (99% ethanol). The samples were then critical-point-dried via liquid CO_2 in a BAL-TEC CPC 030 critical-point-drying apparatus (Balzers, Liechtenstein). The filters were glued onto metal stubs, sputter-coated (90 s, corresponding to 15 nm thickness) with platinum-palladium in a JEOL JFC-2300HR sputter-coater apparatus, and finally examined in a JEOL JSM-6335F Field Emission Scanning Electron Microscope (JEOL, Tokyo, Japan).

TEM. A dense culture was fixed for 1.5 h in cold 2% glutaraldehyde (final concentration) in 0.1 M sodium cacodylate, pH 7.2, containing 0.3 M sucrose to minimize the osmotic change. It was centrifuged (Sigma 302K; Sigma, Osterode/Harz, Germany) into a pellet, which was rinsed over a period of 1.5 h in cold buffer of decreasing sucrose content (0.3, 0.15, and 0 M) before postosmication overnight in cold 1% osmium tetroxide. The pellet was then rinsed quickly in distilled water and dehydrated in an alcohol series (15–20 min in each change of cold 30, 50, 70, and 96% ethanol), brought to room temperature, and dehydrated further in absolute ethanol for 25 min (two changes), followed by propylene oxide for 20 min (two changes). Embedding was in Spurr's embedding medium. The material was left overnight in a 1:1 mixture of propylene oxide and Spurr's mixture in the hood, transferred to 100% Spurr's, left for 4 h at room temperature, and finally polymerized overnight in a fresh mixture of Spurr's at 75°C. Ultrathin sections were cut on an LKB 2088 Ultratome V ultramicrotome (LKB; Bromma, Stockholm, Sweden), mounted on Formvar film on single-hole slot grids, and double stained in 2% methanolic uranyl acetate followed by Reynold's lead citrate, ~20 min in each staining solution. The sections were examined in a JEM-1010 transmission electron microscope (JEOL) and photographed with a Gatan 792 digital camera (Gatan Inc., Pleasanton, CA, USA).

DNA extraction, amplification, and sequencing of nuclear LSU rDNA. Approximately 10 mL of the clonal culture GCTV-B4 was harvested by centrifugation (Sigma-302K; Sigma-Laboratory Centrifuges GmbH, Osterode, Germany) at 2,500 rpm (950*g*) for 10 min. The pellet of cells was transferred to a 1.5 mL Eppendorf tube and frozen at −20°C for 1 week. After thawing, total genomic DNA was extracted using the CTAB (2X hexadecyltrimethyl-ammonium bromide) protocol as previously outlined (Daugbjerg et al. 1994). Partial nuclear-encoded LSU rDNA was amplified in a 50 μL reaction containing 5 μL 10× Taq buffer [67 mM Tris-HCl, pH 8.5, 2 mM $MgCl_2$, 16.6 mM $(NH_4)_2SO_4$, and 10 mM β-mercaptoethanol], 20 μL 0.5 μM dNTP mix, 5 μL 10 μM of each primer, 5 μL 100 mM tetramethylammonium chloride (TMA), and 1 U Taq polymerase (Ampliqon, Herlev, Denmark). Primers for amplification were D1R-F (forward primer) combined with 28-1483 (reverse primer). For primer sequences, see Scholin et al. (1994) and Daugbjerg et al. (2000), respectively. Temperature profile was one initial cycle of denaturation at 94°C followed by 35 cycles where each cycle comprised these steps: denaturation at 94°C for 1 min, annealing at 52°C for 1 min, and extension at 72°C for 3 min. An extension step at 72°C for 6 min ended the temperature profile. The PCR products were run for 15 min at 150 V in a 2% NuSieve gel (NuSieve GTG; BioWhittaker Molecular Applications, Rockland, ME, USA) containing ethidium bromide. To verify that the PCR fragments had the correct length, the gel, including also the molecular marker Phi X175 HAE III (ABgene, IL, Rockford, USA), was placed on a UV light table. Following this check, the PCR fragments were purified using the QIAquick PCR purification kit (Qiagen Inc., Valencia, CA, USA), and 30 ng DNA was used for sequence determination in a 20 μL reaction volume. The LSU rDNA sequence was determined using the dye terminator cycle sequencing ready reaction kit as suggested by the manufacturer (Perkin Elmer, Foster City, CA, USA), and the sequencing reactions were run on an ABI PRISM model 3130 XL automated sequencer (Applied Biosystems, Foster City, CA, USA). Approximately 1,400 bp were determined in both directions using the two amplification primers in addition to the following three internal primers: D3A, D3B, and D2C (Scholin et al. 1994, Nunn et al. 1996).

Alignment and phylogenetic analyses. The gymnodinioid nature of strain GCTV-B4 was confirmed in a nucleotide sequence BLAST in GenBank showing it to be most similar to a sequence of *G. aureolum* (strain KA2) given the accession number DQ917486. This relationship was also confirmed when adding the LSU rDNA sequence of *G. corollarium* [GCTV-B4] to a data matrix comprising a diverse assemblage of naked and thecate dinoflagellates (25 genera and 48 species). Phylogenetic analyses of this data matrix with 1,086 bp of LSU rDNA revealed that *G. corollarium* [GCTV-B4] formed a sister taxon to *G. aureolum* (tree not shown). This information led us to establish a second data matrix consisting of mostly *Gymnodinium* species and several related naked genera (i.e., *Polykrikos*, *Phaeopolykrikos,* and *Lepidodinium*). See Table S1 (in the supplementary material) for a complete list of the species that were included in the phylogenetic analyses. This LSU rDNA data matrix was aligned using ClustalW (Thompson et al. 1994) and further edited by eye using BioEdit ver 7.08 (Hall 2006). The hypervariable domain D2 sensu Lenaers et al. (1989) was partly excluded due to ambiguous alignment. This left 1,289 bp including introduced gaps for phylogenetic inference of *G. corollarium* [GCTV-B4]. Phylogenetic reconstructions were based on Bayesian analysis (BA), maximum parsimony (MP), and neighbor joining (NJ). Four dinoflagellates assigned to the Kareniaceae constituted the outgroup taxa (viz. *Karlodinium veneficum*, *K. armiger*, *Karenia brevis*, and *K. mikimotoi*). BA used the program MrBayes ver. 3.1.2 (Ronquist and Huelsenbeck 2003), and MP and NJ analyses were performed using PAUP* ver. 4.0b10 (Swofford 2003). A GTR substitution model with base frequencies and substitution rate matrix estimated from the data was invoked in BA. A total of 2 million Markov Chain Monte Carlo generations with four parallel chains (three heated and one cold) were completed. A tree was sampled every 50th generation. When plotting the log likelihood values as a function of generations in a spreadsheet, the lnL values converged at ~ −7,340 after 10,050 generations. This number of generations was used as the burn-in, resulting in 39,800 trees. These were imported into PAUP*, and a 50% majority-rule consensus tree was constructed. For MP bootstrap analyses, a total of 1,000 replications were performed. In bootstrap analyses, nucleotide positions were unordered and equally weighted. Introduced gaps were treated as missing data. The Modeltest program ver. 3.7 (Posada and Crandall 1998) was used to locate the best-fit model for the LSU rDNA aligned sequences by hierarchical likelihood ratio test. The best model was TrNef+I+G with among-sites rate heterogeneity ($\alpha = 0.6499$), an estimated proportion of invariable sites ($I = 0.3601$), and two substitution-rate categories (A–G = 2.5646 and C–T = 5.7201). The TrNef+I+G model was applied to compute dissimilarity values, and the resulting distance matrix to build a tree with the NJ method using PAUP*; 1,000 bootstrap replications were performed.

Pigment analysis. Twenty milliliters of a *G. corollarium* [GCTV-B4] culture was filtered onto a 25 mm 0.2 μm Whatman GF/F filter (Whatman International Ltd., Kent, UK). The filter was placed in a 5 mL syringe fitted with a 0.2 μm filter, and 2.5 mL methanol was added. Cells were ultrasonicated with a 6 mm probe for 30 s and filtered into a glass vial from which 1 mL was transferred into a HPLC glass vial containing 250 μL Millipore water. The sample was analyzed by a Waters HPLC system, which included a Waters 600 Controller, a 717 plus Autosampler, and a Waters 996 Photodiode Array Detector (Waters Corp., Milford, MA, USA). Pigments were identified by retention times and absorption spectra identical to those of standards. Pigments were quantified against standards purchased from the International Agency for 14C Determination, Hoersholm, Denmark.

Salinity and temperature tolerance experiment. Salinity and temperature tolerance of *G. corollarium* were studied by growing strain GCTV-B4 at different salinities and temperatures. For the salinity tolerance experiment, cells originally maintained at a salinity of 6 were successively transferred into salinities of 3, 1.5,

and 0; and 9, 12, 15, 20, 25, and 30, respectively. To obtain the lower salinities, medium with a salinity of 6 was diluted with MWC medium (Guillard and Lorenzen 1972). For higher salinities, medium with a salinity of 30 was diluted with local seawater medium (salinity of 6). When an inoculum culture had entered exponential growth phase at a given salinity (typically after 15 to 30 d, depending on the salinity), subsamples were inoculated at initial concentrations of ~350 cells · mL^{-1} to three replicate 50 mL polystyrene tissue culture flasks, each containing 30 mL of f/2—Si medium at the next salinity level. Cultures were allowed to adapt to the new salinity for 1 week before samples were collected for initial measurements. Subsamples for cell counts were taken every 2–5 d, fixed with Lugol's solution, and examined under an inverted light microscope (Leica DMIL or Leica DM IRB; Leica Microsystems GmbH, Wetzlar, Germany). For the temperature tolerance experiment, cultures were successively transferred from maintenance temperature of 4°C to 2°C and 0°C, and 6, 8, and 10°C, respectively, and growth experiments at each temperature were carried out in a similar manner as described above. Each salinity and temperature treatment was monitored until reaching the stationary phase, and maximum number of divisions per day (k) was determined for the exponential growth phase, using the formula $k = [\ln(N_t/N_0)/\Delta t]/0.6931$, where N_0 is the population size at the beginning of a time interval, N_t is the population size at the end of the time interval, and Δt is the length of the time interval. Statistical analyses (one-way analysis of variance [ANOVA]) were performed using STATISTICA software (StatSoft Inc., Tulsa, OK, USA).

Identification of cysts from sediment trap material. Settled material containing cysts resembling the type formed in cultures of strain GCTV-B4 was collected during spring 2006 by a sedimentation trap (Model K/MT234; K.U.M., Kiel, Germany) moored at 180 m depth east of Gotland in the central Baltic proper (station BY15, 57°18.3′ N, 20°04.6′ E, Fig. 1).

The morphology of the sediment trap cysts was examined by LM and SEM. For SEM, a formalin-preserved subsample of settled material was filtered through a Coastar nuclepore polycarbonate membrane filter with a pore size of 2 μm and critical-point-dried via liquid CO_2 in a BAL-TEC CPC 030 apparatus. The filter was fixed onto an aluminum stub and then sputter-coated with gold-palladium (4 min, 25 pm layer) in an EMITECH K950X sputter-coater apparatus (EM Technologies Ltd., Kent, UK). Microphotographs were taken with a SEM Quanta 400 (FEI, Hillsboro, OR, USA). Light micrographs of formalin-preserved sediment trap material were taken at 400× magnification using a Zeiss Axiovert S100 inverted light microscope equipped with a digital camera Olympus DP10.

To establish cultures for DNA comparison of sediment trap cysts and clone GCTV-B4, a subsample of living material from the nonpreserved volume of the trap was suspended in filtered seawater and sonicated for 7 min in an ultrasonic bath (Branson 2200; Branson Ultrasonics Co., Danbury, CT, USA) to clean cysts from attached organic debris. The sample was rinsed through a 50 μm net and concentrated on a 10 μm nylon sieve. From the resulting 10–50 μm fraction, single cysts were isolated into a drop of autoclaved filtered seawater using a micropipette. Single isolated cysts were rinsed several times in separate drops of water before they were placed into 10 mL test tubes filled with 5 mL of diluted f/20-Si medium with a salinity of 6. The tubes were incubated at 4°C, 50 μmol photons · m^{-2} · s^{-1} at a 14:10 L:D cycle until cysts had germinated and strains had reached visible cell densities. The newly established cultures were maintained under the conditions described above.

For DNA analyses, exponentially growing cultures of cyst strains GCTV-01 and GCTV-04 were harvested by centrifugation at 2,500 rpm (1,000*g*) for 5 min. Total genomic DNA was extracted using DNeasy Plant Mini Kit (Qiagen) according to the manufacturer's instructions. Partial LSU rDNA including the D1 and D2 domains was amplified by PCR using primers D1R and D2C (Scholin et al. 1994) and settings specified in Lilly et al. (2005). Purified products were sequenced on an automated sequencer 3730 × l (Applied Biosystems) using the Big DyeTM terminator (Applied Biosystems) cycling conditions. The sequences of the two strains were compared among each other and to the sequence of the cell isolate GCTV-B4 using Clustal W.

RESULTS

Gymnodinium corollarium A. M. Sundström, Kremp et Daugbjerg sp. nov.

Division: Dinoflagellata Fensome et al. 1993
Class: Dinophyceae Pascher 1914
Order: Gymnodiniales Apstein 1909
Family: Gymnodiniaceae Lank. 1885
Genus: *Gymnodinium* F. Stein 1878

Diagnosis: Cellulae vegetativae 20–31 μm longae, 16–24 μm latae, dorsoventraliter paululum compressae. Epiconus subconicus, hypoconus autem rotundatus figura polygonia in amphiesmate conspicua. Apex sulco arcuato et parvis tuberibus ornato ex tribus partibus sinistrorsum cingitur. Cingulum descendens medium spatio suae latitudinis inferius demotum est. Sulcus dimidia parte ad epiconum pertinet, in hypocono ad antapicem versus extenditur, a dextra iugo ventrali insigni terminatur. Flagellum in longitudinem patens per spatium brevius longitudine cellulae corpus occupat. Chloroplasti cellularum ovales, concavi, aureo-fusci non in peripheria dispositi sunt, sed a media cellula radiorum instar proficiscuntur. Pyrenoides adest. Nucleus sphaericus dinocaryo solito in dextro latere dorsali sito. Cystes ovales cum pariete perlucido partibus superficialibus carent. Cystes cellulis vegetativis minores sunt.

Vegetative cells 20–31 μm long, 16–24 μm wide. Cells slightly dorsoventrally compressed. Epicone slightly conical. Hypocone rounded. Polygonal pattern in the amphiesma. Horseshoe-shaped apical groove running anticlockwise 3/4 around the apex; apical groove ornamented with small knobs. Cingulum median descending with a displacement of one width. Sulcus reaching halfway into the epicone; broadening in hypocone toward the antapex; delimited to the right by a pronounced ventral ridge. Longitudinal flagellum trailing body by less than one cell length. Numerous oval and concave shaped golden-brown chloroplasts; nonperipheral radiating from the center of the cell. Pyrenoid present. Nucleus spherical, typical dinokaryon located on the dorsal right side. Oval cysts with transparent cyst wall and no surface structures. Cysts smaller than vegetative cells.

Holotype: Figure 3A. The corresponding clonal culture, strain GCTV-B4, is deposited at Tvärminne Zoological Station, University of Helsinki, Hanko, Finland, and at the Scandinavian Culture Centre for Algae and Protozoa, Department of Biology,

University of Copenhagen, Denmark. Here it was given the strain number SCCAP K-0983.

Type locality: Station BY29 (58°53′ N, 20°19′ E), northern Baltic proper, Baltic Sea, Sweden (Fig. 1).

Etymology: Named after the garland (=*corollarium*) shaped appearance of the chloroplasts as observed under the light microscope in midfocus.

Morphology: The general features of the morphology of *G. corollarium* sp. nov. are shown in Figures 2 and 3. Exponentially growing cells are 20.0–31.3 μm long (mean = 25.6 μm, SD ± 2.6 μm, $n = 20$) and 16.3–23.8 μm wide (mean = 19.9 μm, SD ± 1.9, $n = 20$). Their average body width/length ratio is 0.8 (SD ± 0.0, $n = 20$), ranging from 0.7–0.9 μm.

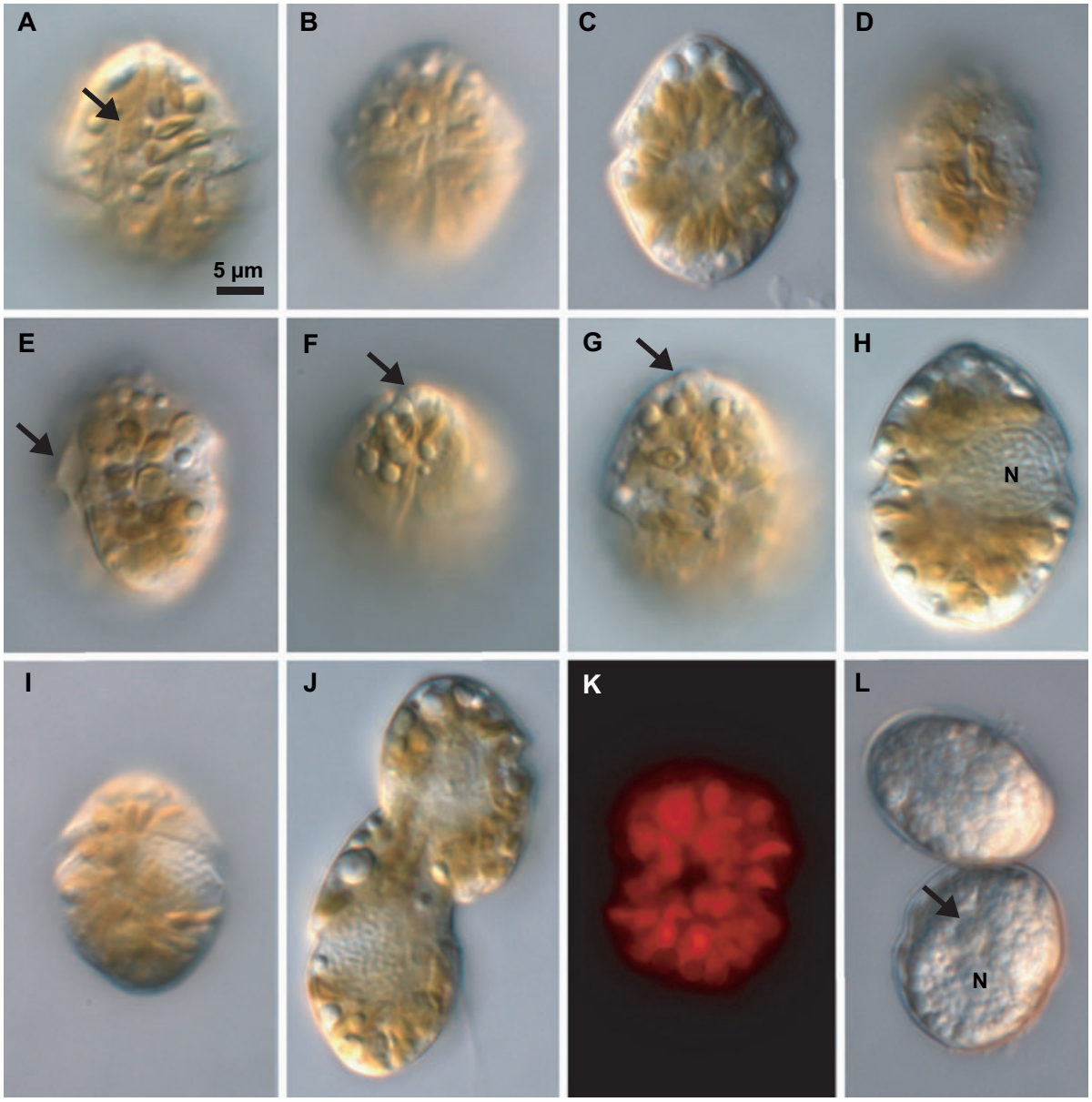

FIG. 2. Light micrographs of *Gymnodinium corollarium* [GCTV-B4]. The scale is the same for all pictures. (A) Ventral view showing the cingular displacement, the sulcal extension (arrow), the ventral ridge, and the oval concave chloroplasts. (B) Ventral view showing the displaced cingulum, the sulcus, the ventral ridge, the sulcal extension, and the apical groove. (C) Central focus showing the arrangement of the oval concave chloroplasts. (D) Left side of the cell showing the distinct median cingulum. (E) Sinistroventral view showing the very distinct ventral ridge (arrow). (F) View from ventral apex displaying the ventral ridge, the sulcal extension, and the apical groove (arrow). (G) Ventral view with indicated apical groove (arrow). (H) Dorsal midway view showing the right-sided nucleus (N) and numerous chloroplasts. (I) Dorsal surface view with the nucleus on the right side close to the cingulum. (J) Dividing cells. The nucleii and the longitudinal flagellum are displayed. (K) Epifluorescence microscopy displaying profiles of numerous chloroplasts. (L) Resting cysts showing the cyst wall, the nucleus (N), and the residual bodies (arrow).

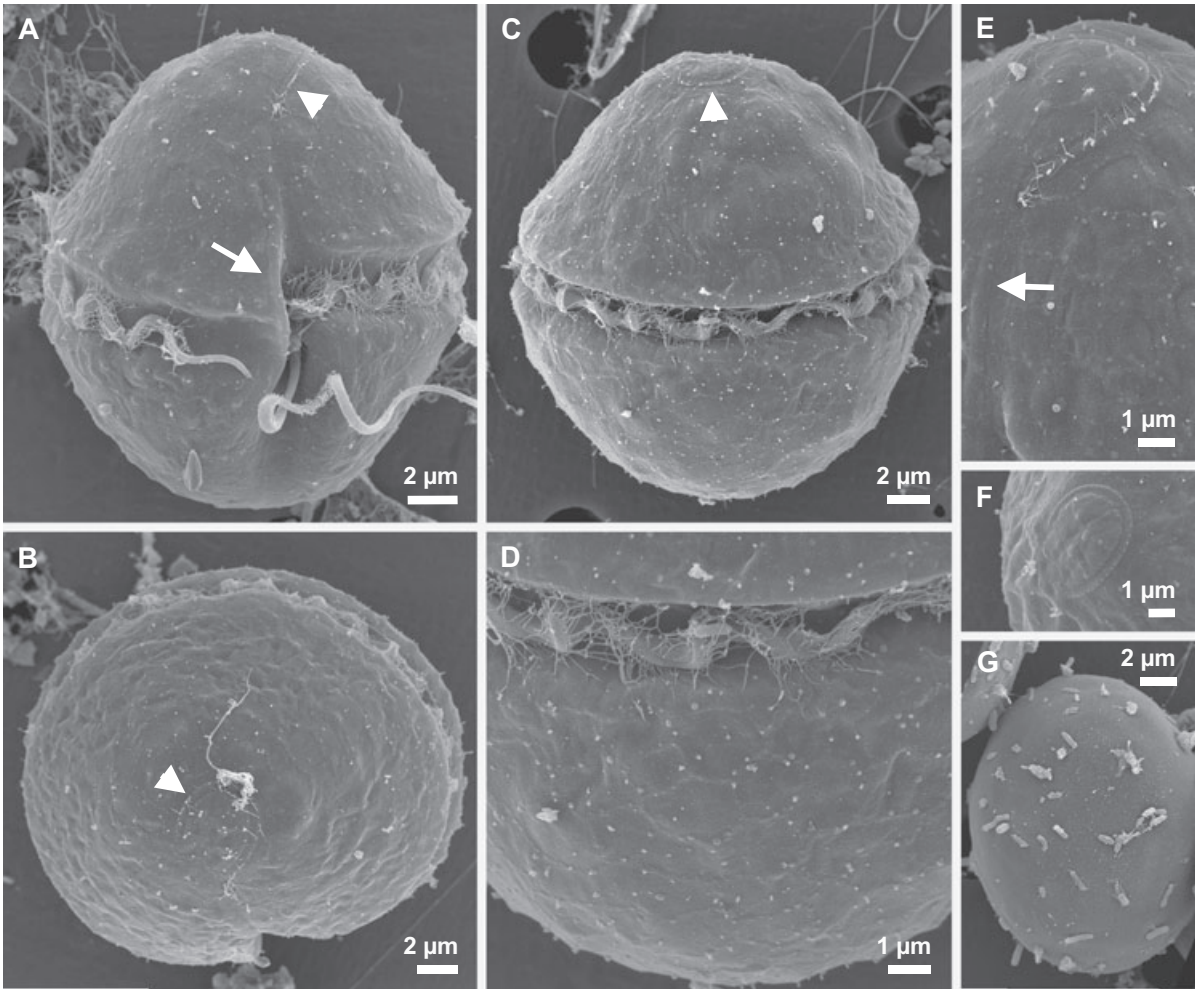

FIG. 3. SEM micrographs of *Gymnodinium corollarium* [GCTV-B4]. (A–F) Vegetative cells. (G) Resting cyst. (A) Ventral view showing the displacement of the cingulum, the sulcus, the sulcal extension, the apical groove (arrowhead), and the wall-like structure of the ventral ridge (arrow). Transverse flagellum and longitudinal flagellum are also displayed. (B) Apical view with apical groove (arrowhead). (C) Dorsal view showing the median placement of cingulum, the transverse flagellum, and the apical groove (arrowhead). (D) Polygonal pattern of the amphiesma. The transverse flagellum is displayed. (E) Sulcal extension (arrow) and apical groove. (F) Close view of the apical groove ornamented with small knobs. (G) Oval and smooth resting cyst with bacteria attached to the surface.

Cells of *G. corollarium* are ovoid in shape and somewhat dorsoventrally compressed (Figs. 2 and 3). Their epicone is usually conical compared to the hypocone, which generally appears more hemispherical (Figs. 2, A–C, and 3, A–C). The amphiesma of the cell has a polygonal pattern (Fig. 3D), which was not visible in the sulcal area. The cingulum is median (Figs. 2, B–D, and 3, A, C), has well-defined edges, and circles counterclockwise around the cell down to the right side, resulting in a displacement of approximately one cingular width (Figs. 2, A, B, and 3A). The sulcus broadens into the hypocone and also extends as a narrow furrow into the epicone, where it nearly connects to the onset of the distinct apical groove (Figs. 2B and 3A). To the right, the sulcus is delineated by a pronounced ventral ridge, which has a slightly sigmoid outline when seen in ventral view (Figs. 2, A, E, and F, and 3A). The horseshoe-shaped apical groove runs from the end of the sulcal extension counterclockwise around the apex, ending at the right side of the cell and hence leaving a broad opening to the ''horseshoe'' (Figs. 2, B, F, and G, and 3, A–C, E, and F). The apical groove was found to be ornamented with small knobs (Fig. 3F).

The spherical nucleus is situated on the right dorsal side of the cell just beneath the cingulum (Fig. 2, H, I). Figure 2J shows a dividing cell pair. *G. corollarium* divides by binary fission while swimming. Oblique division begins by an invagination of the posterior end of the mother cell. The chloroplasts as seen in interference contrast LM are yellow-brown and have an oval and concave shape (Fig. 2, A, C, E, and H). They are withdrawn from the periphery of the cell and appear to radiate from the central part (Fig. 2C). Epifluorescence microscopy revealed more than 20 chloroplasts in the cells during exponential growth (Fig. 2K). Resting cysts

are usually formed in large amounts in nutrient-deplete cultures. The oval cysts, which have transparent walls, are much smaller than the flagellate cells. Length measurements of GCTV-B4 cysts ranged from 13.5 to 22.1 μm (mean = 17.5 μm, SD ± 2.0 μm, $n = 20$), and cysts are 9.9–16.5 μm wide (mean 13.7 μm, SD ± 1.4 μm, $n = 20$). The colorless cysts contain numerous starch grains and a yellow-greenish residual body (Fig. 2L). The nucleus is often visible under LM. The cyst wall is relatively thick and may appear somewhat irregular. However, the surface of the cyst wall is smooth with no visible structures (Figs. 2L and 3G).

Ultrastructure. Some details of the cell ultrastructure are illustrated in Figure 4, A–C. The centrally located compound pyrenoid with branches extending toward the cell periphery is illustrated in Figure 4A. The nuclear envelope was examined in detail to determine whether nuclear chambers were present, and while these were initially difficult to see, they were eventually found in better-fixed material as illustrated in Figure 4B. The cells also contained trichocysts of typical dinoflagellate morphology (Fig. 4C). The trichocysts have mucus-like vesicles located on the sides. The amphiesmal vesicles contain a thin plate (Fig. 4C).

Phylogeny of Gymnodinum corollarium *[GCTV-B4] based on partial LSU rDNA.* Figure 5 shows the phylogenetic inference based on BA. The tree topology revealed that *G. corollarium* strain GCTV-B4 was related to two isolates of *G. aureolum* from the U.S. (strains KA2 and S1-30-6, respectively). However, this relationship only received moderate support (posterior probabilities = 0.64 and MP bootstrap analyses = 60%). The relationship received <50% support in NJ bootstrap analyses. *G. corollarium* [GCTV-B4] and the U.S. isolates of *G. aureolum* grouped with the type species of *Gymnodinium* (viz. *G. fuscum*), *G. palustre*, *G. venator*, and *Dissodinium pseudolunula*. This clade received a posterior probability of 0.96 but <50% bootstrap support in MP and NJ. The three methods applied to reconstruct the phylogeny of *G. corollarium* [GCTV-B4] all indicate that the genus *Gymnodinium* is polyphyletic, as *Lepidodinium* spp., *Polykrikos* spp., and *Phaeopolykrikos hartmannii* cluster within species of *Gymnodinium* (see comment on the relationship of *G. aureolum* strain GrAr01 below).

Sequence divergence. PAUP* was used to estimate the sequence divergence between *G. corollarium* [GCTV-B4] and the six most closely related species as suggested by the phylogenetic reconstruction shown in Figure 5. The sequence comparison was based on 1,289 bp. Depending on the method used to estimate the sequence divergence, a difference of 4.04%–7.62% between *G. corollarium* sp. nov. (GCTV-B4) and the U.S. isolates of *G. aureolum* was obtained (Table 1). The sequence divergence between *G. corollarium* sp. nov. and the type species of *Gymnodinum* (viz. *G. fuscum*) was slightly higher (9.31%–10.03%), whereas it differed by ~6.5% to *Dissodinium pseudolunula*, a parasitic dinoflagellate on copepod eggs (Drebes 1978). The sequence divergence between *G. aureolum* strain GrAr01 and the U.S. isolates of *G. aureolum* (strains KA2 and S1-30-6, respectively) was 11%–15% (Table 1).

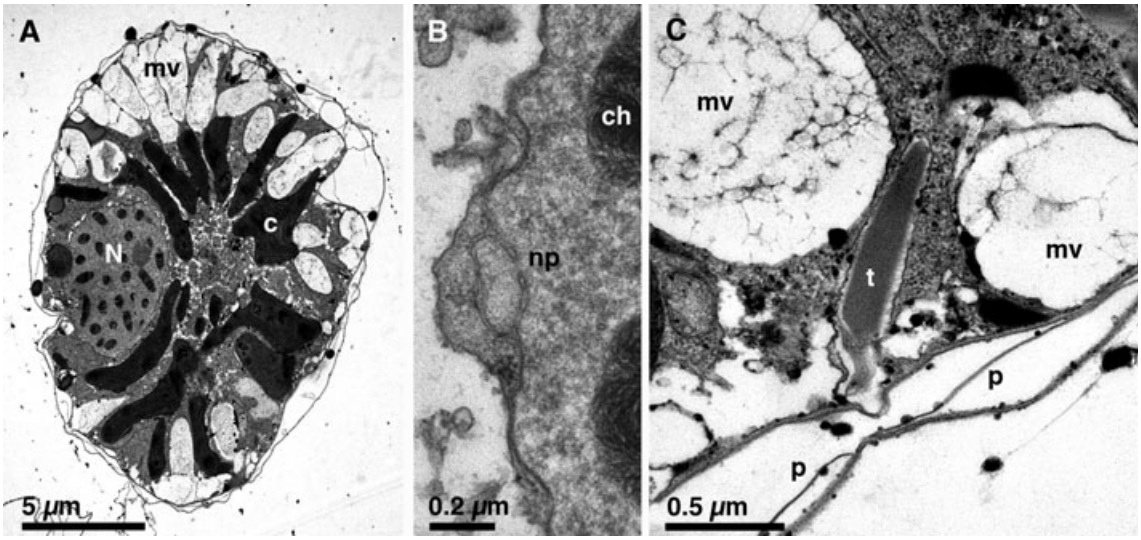

FIG. 4. TEM micrographs of *Gymnodinium corollarium* [GCTV-B4]. (A) Oblique section revealing the general disposition of major organelles. Note chloroplast lobes (c) radiating from the central area toward the cell perimeter. Numerous vacuoles with mucus-like material (mv) are seen at the cell periphery. Nucleus (N). (B) High magnification of parts of the nuclear envelope. A nuclear chamber with a nuclear pore (np) is indicated. Note chromosomes (ch) to the right. (C) High magnification of cell perimeter revealing a longitudinally sectioned trichocyst (t) and a thin plate (p) in the amphiesmal vesicles. Mucus-like vesicles (mv) are located on each side of this trichocyst.

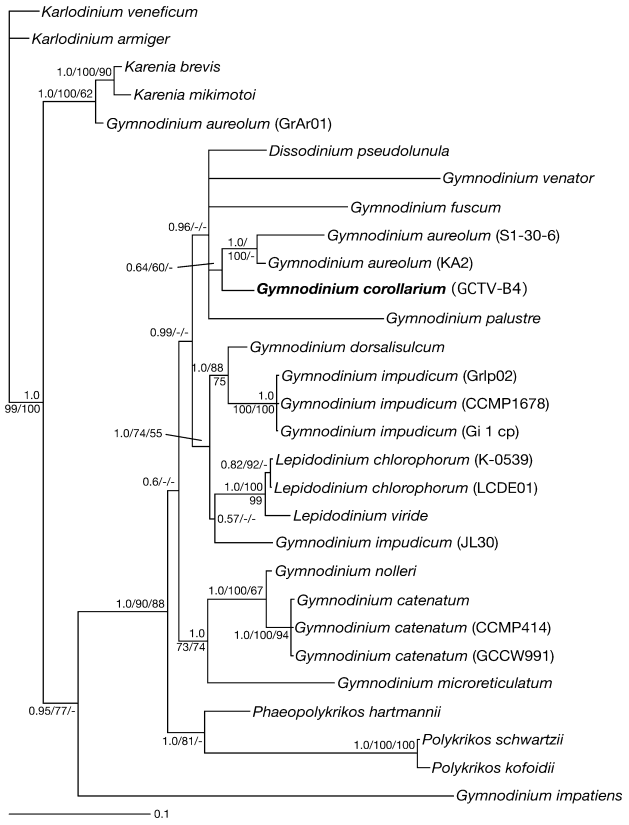

FIG. 5. Phylogeny of *Gymnodinium corollarium* [GCTV-B4] based on Bayesian analysis. The data matrix analyzed included 1,289 bp of the nuclear-encoded LSU rDNA gene. *Karlodinium* spp. and *Karenia* spp. formed the outgroup. Branch support values from posterior probabilities (PP), and bootstrap (BS) are written at internodes. Numbers written first are PP values, followed by BS values (in percent) from maximum parsimony (MP) and neighbor joining(NJ), respectively. Only support values ≥0.5 in Bayesian analysis (BA) or 50% in MP and NJ bootstrap are listed. The branch lengths are proportional to the number of character changes (see scale bar). The LSU rDNA sequence of *G. corollarium* [GCTV-B4] determined in this study is boldfaced.

Hence, *G. aureolum* strain GrAr01 is obviously misidentified, and this was also indicated by the phylogeny shown in Figure 5.

Pigment profile. The HPLC analysis of chloroplast pigments of *G. corollarium* [GCTV-B4] is shown in Figure 6. Chl pigments detected in the cultures were chl *a* and chl c_1/c_2 (not separated by the employed method); carotenoid pigments consisted of peridinin, diadinoxanthin, and β-carotene in small amounts.

Salinity and temperature tolerance. The ANOVA analyses revealed significant differences in growth rate for both the salinity and the temperature treatments ($P < 0.001$ and $P < 0.001$, respectively). Cultures of strain GCTV-B4 grew well in salinities up to 25 (Fig. 7A). *G. corollarium* grew best in salinities between 1.5 and 12 ($k = 0.41$–0.51 divisions $\cdot$ d^{-1}) with a growth optimum at a salinity of 9 ($k = 0.51$ divisions $\cdot$ d^{-1}). In a salinity of 30, only weak growth was observed. Initial growth was also observed in freshwater media. However, in this treatment, the population started to decrease after 4 weeks. *G. corollarium* grows well in temperatures between 2°C and 6°C ($k = 0.42$–0.47 divisions $\cdot$ d^{-1}, Fig. 7B); optimum temperature for growth was 4°C ($k = 0.47$ divisions $\cdot$ d^{-1}). High growth rates were also observed at 0°C, but growth performance was poor at 8°C and 10°C, where only small increases in cell abundances were observed.

Sediment trap cysts. Large numbers of cysts (Fig. 8), resembling the cysts formed routinely by the GCTV-B4 isolate of *G. corollarium* (Figs. 2L and 3G) were found in the sediment traps. The transparent ovoid cysts were 15–20 μm long and had a smooth wall. Their shape was typically more irregular than the shape of cysts produced in culture, and often the characteristic dinoflagellate shape with cingular grove and sulcal depression was preserved (Fig. 8A). Cells in cultures grown from germinated sediment trap cysts had the same size and shape and typical chloroplast arrangement as *G. corollarium* [GCTV-B4] cells, and DNA comparison revealed identical D1-D2 domains of strain GCTV-B4 and the two examined cyst strains, GCTV-01 and GCTV-04.

DISCUSSION

Taxonomic assignment. This paper describes a hitherto unidentified spring dinoflagellate species from the Baltic Sea. Our results demonstrate that

TABLE 1. Sequence divergence in percentage of *Gymnodinium corollarium* and the closely related *G. aureolum* (three strains), *G. fuscum, G. venator,* and *Dissodinium pseudolunula* based on 1,289 bp of nuclear-encoded LSU rDNA.

	Gymnodiniums corollarium (GCTV-B4)	*Gymnodinium aureolum* (KA2)	*Gymnodinium aureolum* (S1-30-6)	*Gymnodinium aureolum* (GrAr01)	*Gymnodinium fuscum* (CCMP1677)	*Gymndinium venator*	*Dissodinium pseudolunula* (JHW0205-1)
G. corollarium (GCTV-B4)	–	4.04	7.22	9.93	9.31	11.52	6.4
G. aureolum (KA2)	4.17	–	3.97	10.96	9.54	12.08	6.86
G. aureolum (S1-30-6)	7.62	4.08	–	13.42	12.56	14.70	6.73
G. aureolum (GrAr01)	10.69	11.93	14.94	–	13.14	15.99	13.37
G. fuscum (CCMP1677)	10.03	10.3	13.88	14.55	–	14.65	11.02
G. venator	12.66	13.36	16.59	18.29	16.62	–	15.20
D. *pseudolunula* (JHW0205-1)	6.71	7.22	7.07	14.82	12.08	17.27	–

Uncorrected distances (''p''-values in PAUP*) are given above the diagonal, and distance values using Kimura 2-parameter model are given below the diagonal.

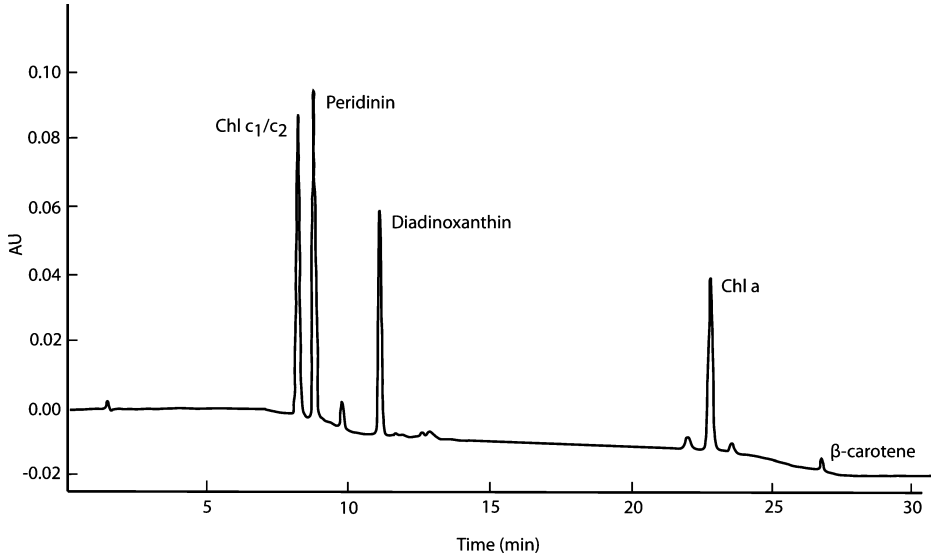

FIG. 6. High-performance liquid chromatogram of extracted pigments from *Gymnodinium corollarium* [GCTV-B4].

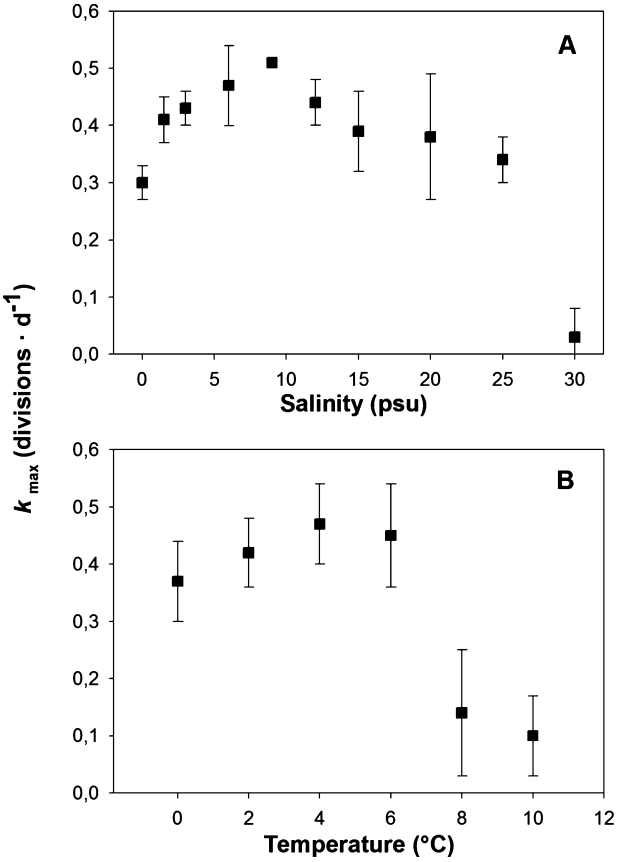

FIG. 7. Division rates (k) of *Gymnodinium corollarium* at different (A) salinities and (B) temperatures. Error bars = standard deviations (n = 3).

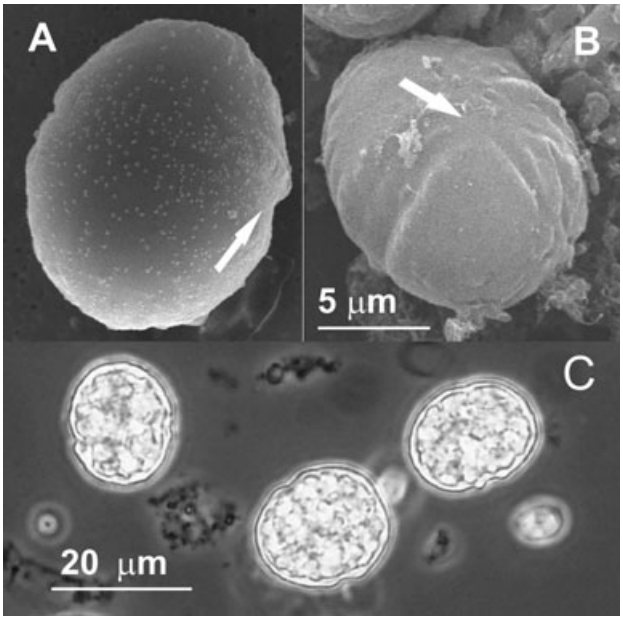

FIG. 8. Sediment trap cysts produced by *Gymnodinium corollarium*. (A) SEM of a cyst collected from Gotland Sea and prepared by air drying. (B) SEM of cyst from a Gotland Sea sample (critical-point-dried). (C) LM of formalin-preserved cells in a sediment trap sample from the Gotland Sea. Arrows mark paracingulum (A) and parasulcus (B). The scale of (A) and (B) is the same.

G. corollarium sp. nov., to which we assign this dinoflagellate, is a novel species. It differs from all other *Gymnodinium* species reported so far from the Baltic Sea (Hällfors 2004) and elsewhere (Schilling 1891, Kofoid and Sweezy 1921). Morphological and ultrastructural features in this species, such as a horseshoe-shaped apical groove running in a counterclockwise direction around the apex, a cingulum displacement of one cingulum width, and the presence of nuclear chambers in the nuclear envelope, place it in the genus *Gymnodinium* as redefined by Daugbjerg et al. (2000) (whether a nuclear connective is present is not known). Species identification within this genus is based on shape and size of cells, chain formation or single cell habitus, sulcal extensions, surface structures, placement of the nucleus, presence of chloroplasts, and pigment composition. However, differences in such characters can be subtle,

making it difficult to identify a species reliably. In the case of *G. corollarium*, molecular phylogenetic analyses helped to segregate this species from some morphologically similar species—such as *G. nolleri, G. catenatum, G. microreticulatum, G. impudicum*—and identify the close or potentially conspecific relatives. In the comparison of LSU rDNA sequences, *G. corollarium* clustered together with *G. fuscum*, *G. venator*, *G. palustre*, *Dissodinium pseudolunula,* and *G. aureolum*. While conspecificity with the first four of these can be excluded due to pronounced differences in body size and shape, position of the nucleus, life-form, and habitat (Table 2), separation from *G. aureolum* may not be immediately obvious.

Despite the general resemblance and close genetic relationship to *G. aureolum*, distinct morphological differences—such as the nonperipheral arrangement of the chloroplasts, the right dorsal position of the nucleus, the comparatively short apical groove, and the pronounced ventral ridge—clearly separate *G. corollarium* from the latter. The recognition of *G. corollarium* as a distinct species is further supported by the presence of a specific cyst type, which is small and may display features from the vegetative stage, such as well-defined paracingular and parasulcal regions. According to the size ranges given by Hulburt (1957) and Hansen et al. (2000a), *G. aureolum* is somewhat larger than *G. corollarium*. However, Tang et al. (2008) observed considerable variations in cell size for *G. aureolum*; *G. corollarium* also varies in cell size depending on life- and cell-cycle stage and fits into the broad size interval of *G. aureolum*. The cell shape is highly similar between the species; both have a slightly sigmoid ventral ridge, although the one of *G. corollarium* to a lower degree. The ventral ridge in both species terminates into a small projection; however, in *G. corollarium,* the ventral ridge sometimes forms a distinct wall-like structure together with the cingulum-sulcus border. Moreover, in *G. aureolum,* the sulcus extends all the way to the antapex (Hansen et al. 2000a, Tang et al. 2008), resulting in an antapical indentation, whereas in *G. corollarium,* the sulcus only extends 3/4 into the hypocone, thus leaving the antapex rounded. Both species have a horseshoe-shaped apical groove encircling the apex in a counterclockwise direction. However, in *G. aureolum,* it encircles the apex nearly entirely (Hansen et al. 2000a), whereas the apical groove of *G. corollarium* only runs ~3/4 around the apex, leaving the opening of the ''horseshoe'' wide open. Furthermore, the fine structure of the apical groove is different in the two species: in contrast to *G. corollarium* where small knobs line the outer edge of the groove, the acrobase of *G. aureolum* consists of two parallel grooves on both sides of a central ridge (Tang et al. 2008). The presence of apical knobs in the acrobase appears to be a widespread feature in thin-walled or naked dinoflagellates and can, for example, be seen in the woloszynskioids *Tovellia coronata* (Lindberg et al. 2005), *Biecheleria pseudopalustris* (Moestrup et al. 2009a), and *Biecheleriopsis adriatica* (Moestrup et al. 2009b). This feature also occurs in the gymnodinioids *Gyrodinium vorax* and *Gymnodinium maguellonnense* (Biecheler 1952).

Hansen et al. (2000a) did not describe any surface patterns on *G. aureolum*. Conversely, Tang et al. (2008) observed a polygonal pattern on the cell surface reflecting the polygonal arrangement of the amphiesmal vesicles, a feature also found in *G. corollarium*. Chloroplast structure and arrangement of *G. aureolum* may differ between strains (Hansen et al. 2000a, Tang et al. 2008). However, the numerous chloroplasts of *G. corollarium* are uniquely withdrawn from the periphery of the cell, a feature not encountered previously within the genus *Gymnodinium*. They extend from a compound pyrenoid located centrally in the cell. Peridinin is the major carotenoid in both species (Hansen et al. 2000a). The presence of nuclear chambers is characteristic of the *Gymnodinium* clade, but their functional significance is still unknown (Daugbjerg et al. 2000, Hansen et al. 2000a). The cysts of *G. aureolum* are microreticulate and surrounded by mucus (Hansen et al. 2000a, Tang et al. 2008), but these features were never observed on *G. corollarium* cysts.

For a number of species belonging to the *Gymnodinium* sensu stricto group (Daugbjerg et al. 2000), molecular data are not available, and comparison of such species to *G. corollarium* is limited to morphological features. Although *G. corollarium* shares some features with *G. acidotum*, *G. allophron*, *G. cryophilum*, *G. limitatum*, and *G. maguelonnense*, there is no complete overlap with any species that could indicate conspecificity (Table 2). Wilcox and Wedemayer (1984) determined that *G. acidotum* also has polygonal vesicles underneath the plasmalemma, but corresponding surface structures have not been confirmed. Motile cells of *G. acidotum* are considerably larger and differently shaped from cells of *G. corollarium*, with both epicone and hypocone being pointed. Moreover, the chloroplasts of *G. acidotum* are endosymbiotic (Wilcox and Wedemayer 1984). *G. allophron* is similar in size, although slightly more elongated (Larsen 1994). However, *G. allophron* is a heterotrophic species, and its apical groove encircles the apex nearly entirely. *G. cryophilum* is similar in size and shares the polygonal amphiesmal pattern, the presence of numerous golden-yellow chloroplasts, and the preference for cold water with *G. corollarium* (Wedemayer et al. 1982, Wilcox et al. 1982). However, it is a freshwater species and differs from *G. corollarium* by its short epicone and the position of the nucleus, which is located in the hypocone. Phototrophic *G. limitatum* (Skuja 1956) is of approximately the same size and shape as *G. corollarium,* and its nucleus is, like in *G. corollarium*, positioned laterally in the epicone. The chloroplasts of *G. limitatum* also radiate from the center to the

TABLE 2. Comparison of characters between *Gymnodinium corollarium* and species of taxonomical interest.

Species	Length (μm)	Width (μm)	Cell surface	Apical groove	Chloroplasts	Nucleus position	Habitat preference	Cyst morphology
Gymnodinium corollarium	20–31	16–24	Polygonal pattern in amphiesma	Encircling apex to 3/4, ornamented with apical knobs	Numerous; non-peripheral, radiate from center	Dorsal, right side	Brackish	Oval, transparent cyst wall, no surface structures (sometimes shaped like the vegetative cell)
Gymnodinium aureolum[a]	27–34 19–39 14–47	17–32 14–33 11–43	Smooth/polygonal pattern in amphiesma	Encircling apex nearly completely, consists of two parallel tracks	Numerous; radially arranged (or probably one large branching)	Central/in epicone	Marine	Spherical/ovoid, colorless, microreticulate ornamentation, surrounded by mucus
Gymnodinium fuscum[b]	80–100 50–70 50–80	55–60 30–38	Surface striae on the cell	Encircling apex to ca. 3/4	Numerous small; radially arranged (possibly one large reticulated)	Dorsal, in epicone	Freshwater	Hexa- or pentagonal pattern on cyst wall
Gymnodinium venator[c]	n. a.		No surface features	Encircling apex	Heterotrophic	Anterior	n. a.	n. a.
Dissodinium pseudolunula[d]	23–28	18–21	n. a.	n. a.	Heterotrophic/parasitic	n. a.	Marine/ brackish water	Primary cyst spherical, secondary cyst lunate
Gymnodinium palustre[e]	45	37	No structures visible	n. a.	Numerous, peripheral	n. a.	Freshwater	Spherical, enveloped in multilayered mucilage/ thick membrane
Gymnodinium acidotum[f]	33–37	24–30	No surface features (=smooth?)	Encircling apex	Few lobed, constituted by the endosymbiont	Central	Freshwater	n. a.
Gymnodinium cryophilum[g]	33 (mean)	22 (mean)	Polygonal pattern in amphiesma	Encircling apex	Numerous, peripheral	In hypocone	Freshwater	Forms cyst-like structures
Gymnodinium allophron[h]	20–30	12–19	n. a.	Encircling apex nearly completely	Heterotrophic	In hypocone	Marine	n. a.
Gymnodinium limitatum[i]	24–38	20–34	n.a.	n.a.	Numerous rod shaped, radiating from center	In hypocone	Freshwater	Cysts spherical, covered with mucilage
Gymnodinium maguelonnense[j]	34–42	28–40	Polygonal pattern in amphiesma	Encircling apex nearly completely, apical knobs present	Numerous lamellate, radiating from center	Central, dorsal side	Freshwater	n. a.

n. a., data not available.
[a]Daugbjerg et al. 2000, Hulburt 1957, Hansen et al. 2000a, Hansen 2001, Tang et al. 2008.
[b]Daugbjerg et al. 2000, Dodge and Crawford 1969, Ehrenberg 1834, 1838, Hansen et al. 2000b, Schiller 1932, Stein 1883.
[c]Flø Jørgensen et al. 2004, Herdman 1922, Murray and Patterson 2002.
[d]Elbrächter and Drebes 1978, Swift 1973.
[e]Schilling 1891.
[f]Daugbjerg et al. 2000, Nygaard 1949, Wilcox and Wedemayer 1984.
[g]Daugbjerg et al. 2000, Wedemayer et al. 1982, Wilcox et al. 1982.
[h]Larsen 1994.
[i]Skuja 1956.
[j]Biecheler 1939, 1952.

periphery of the cell, but in contrast to *G. corollarium*, they are long and rod shaped. Furthermore, in *G. limitatum*, the sulcal extension into the epicone is tilted to the left, which is not the case in *G. corollarium*. *G. limitatum* is a freshwater species typically associated with the warm water community (Skuja 1956). Of the five species mentioned above, *G. maguelonnense* is the one that most closely resembles *G. corollarium*. It has a similar ovoid cell shape, polygonal pattern in the amphiesma, presence of small knobs in the acrobase, and dorsal position of the nucleus (Biecheler 1952). However, the motile cells of *G. maguelonnense* are usually larger than the ones of *G. corollarium*. According to Biecheler (1952), the chloroplasts are lamellate, implying that they are longer than in *G. corollarium*. Differences were also recognized in the shape of the apical groove, which resembles a horseshoe but, as in *G. aureolum*, nearly reconnects to its onset at the tip of the sulcal extension. In *G. corollarium*, the apical groove only runs ~3/4 around the apex, leaving the ''horseshoe'' widely open.

Phylogenetic relationships within the genus Gymnodinium. The phylogenetic tree reveals that *G. corollarium* has a close relationship with *G. aureolum*, *G. fuscum*, *G. venator*, *G. palustre*, and *D. pseudolunula*, as they all appear in the same cluster. Of all these species, *G. aureolum* (strains S1-30-6 and KA2) has the closest genetic resemblance to *G. corollarium*. A sequence divergence of 4.04%–7.62%, which is higher than that recorded among closely related but non-conspecific strains (Hansen et al. 2000b), supports the separation as different species. The molecular phylogeny based on LSU rDNA places *G. aureolum* strain GrAr01 in a cluster with several *Karenia* spp. This and the clustering of other *Gymnodinium* spp. within other genera strongly advocate that the current taxonomy of the genus *Gymnodinum* is in need of revision using information from morphology (including ultrastructure) and additional molecular sequence data. This has also been shown previously (e.g., Hansen et al. 2007). Tang et al. (2008) examined the relationship between several strains of *G. aureolum*, which all turned out to indeed belong to this species. Included in their analyses, as well as in ours, were strains KA2 and S1-30-6. The close relationship among all these *G. aureolum* strains reinforces the justification of *G. corollarium* and *G. aureolum* as separate species. Combining the morphological features from LM and EM with the molecular-based phylogeny and sequence divergence estimate, we conclude that *G. corollarium* is related to but clearly distinct from *G. aureolum*.

Four isolates of *G. impudicum* were included, but only three of these formed a monophyletic clade with maximum support from posterior probabilities and bootstrap analyses (1.0% and 100%, respectively). *G. impudicum* strain JL30 clustered with the two species of *Lepidodinium* included (viz. *L. chlorophorum* and *L. viride*). Therefore, the identification of strain JL30 isolated from the Gulf of Naples is in need of reexamination. Three strains identified as *G. aureolum* and available in GenBank were also included in the phylogenetic inference. Two of these were monophyletic, whereas *G. aureolum* strain GrAr01 formed a sister taxon to *Karenia* spp. Based on this relationship and a nucleotide sequence BLAST search, we speculate that *G. aureolum* (GrAr01) is in fact a misidentified *Karenia* (perhaps even a strain of *K. umbella*).

Ecology and distribution. Growth experiments showed that *G. corollarium* is adapted to a narrow window of low temperatures, which indicates that the species is confined to cold water of temperatures between 0°C and 6°C. Although the seasonal cycle of *G. corollarium* is still unexplored, the occurrence of the vegetative cells in a March phytoplankton sample and the high number of its cysts in sediment traps during spring suggest that the species belongs to and probably is an important member of the spring phytoplankton community of the Baltic Sea. Unidentified, medium-sized autotrophic *Gymnodinium* spp. have been regularly reported from the Baltic Sea from spring phytoplankton samples (Niemi 1975, Hobro 1979, Hajdu and Willén 1985, HELCOM 1990, 1996). Such spring dinoflagellates have also been assigned to *Peridinium* sp., *P. hangoei*, and *Glenodinium* sp. due to the identification difficulties in preserved samples (for references see Jaanus et al. 2006). After Larsen et al. (1995) redescribed *Scrippsiella hangoei*, the subdominating spring dinoflagellate species was mostly called *S. hangoei*. The situation became more complicated after Kremp et al. (2005) determined that *S. hangoei* co-occurs with *Woloszynskia halophila*, which is actually the dominating species in the Gulf of Finland. Currently, the two cold-water dinoflagellates *S. hangoei* and *W. halophila*, which have similar temperature requirements (Kremp et al. 2005), are known to bloom at the same time in the northern Baltic Sea. High abundances of the ''*Scrippsiella/Woloszynskia* complex'' have also been regularly reported from the northern Baltic Proper during spring (Jaanus et al. 2006). Possibly, *G. corollarium* has been included in this complex of ovoid, medium-sized autotrophic dinoflagellates due to the similar appearance in Lugol's preserved samples when seen in LM.

The salinity preferences determined in this study clearly show that *G. corollarium* is adapted to brackish water conditions. The species thrives well at salinities up to 25 and can even grow in freshwater. Hence, it could potentially occur in most parts of the Baltic Sea, from the innermost bays of the Bothnian Bay in the North to the Kattegat in the South. Phototrophic, medium-sized *Gymnodinium* spp. have in fact been reported from all over the Baltic including the Kattegat (Thomsen 1992, Hällfors 2004). Illustrations of dinoflagellate cells collected from the southeastern Bothnian Sea in May 1985 strongly resemble *G. corollarium*, particularly as the

TABLE 3. Records of the cyst type now recognized as *Gymnodinium corollarium* in the Baltic Sea (from south to north).

Location	Station code	Year	Sample type	Cyst sedimentation rates/abundances	Source
Bornholm Sea	BY 5	2002	Water sample (48 m)	n. a.	R. Hansen, personal observation
Eastern Gotland Sea	BY 15	1999	Sediment trap (180 m)	$31 \times 10^6 \cdot m^{-2} \cdot d^{-1}$	R. Hansen, personal observation
		2002	Sediment trap (180 m)	$11 \times 10^6 \cdot m^{-2} \cdot d^{-1}$	R. Hansen, personal observation
		2003	Sediment trap (180 m)	$1 \times 10^6 \cdot m^{-2} \cdot d^{-1}$	R. Hansen, personal observation
		2004	Sediment trap (180 m)	$4 \times 10^6 \cdot m^{-2} \cdot d^{-1}$	R. Hansen, personal observation
		2005	Sediment trap (180 m)	very common	R. Hansen, personal observation
		2006	Sediment trap (180 m)	very common	R. Hansen, personal observation
Western Gotland Sea	BY 38	1985	Water sample (0–10 m)	$27 \times 10^3 \cdot L^{-1}$	S. Hajdu, personal observation
Baltic proper	BY 31	1996	Sediment trap (50 m)	$25 \times 10^6 \cdot m^{-2} \cdot d^{-1}$	Höglander et al. (2004)
					H. Höglander, personal communication
Northern Baltic proper	BY 29	1979	Water sample (70 m)	$14.5 \times 10^3 \cdot L^{-1}$	S. Hajdu, personal observation
Åland Sea	F 64	1979	Water sample (0–10 m)	$14.5 \times 10^3 \cdot L^{-1}$	S. Hajdu, personal observation
Bothnian Sea	SR 1A	1980	Water sample (0–10 m)	$3.7 \times 10^3 \cdot L^{-1}$	S. Hajdu, personal observation
Bothnian Bay	RR 5	1980	Water sample (60 m)	$21 \times 10^3 \cdot L^{-1}$	S. Hajdu, personal observation

n. a., data not available.

Records are based on observations in spring samples from the HELCOM phytoplankton and sedimentation monitoring program. Cyst sedimentation rates estimated from sediment traps are given in number of cysts $\cdot m^{-2} \cdot d^{-1}$. Cyst abundances estimated from water samples are given in number of cysts $\cdot L^{-1}$.

chloroplasts were depicted as central, which is the signature feature of this novel species (S. Hajdu, personal observation). Thomsen (1992), on the other hand, observed an unidentified *Gymnodinium* sp. (10–20 μm) in the Kattegat that contributed a major part of the biomass in April 1989. Considering the wide salinity tolerance of *G. corollarium,* it is possible that these records represent this species.

The formation of large amounts of resting cysts in nutrient-deplete cultures suggests that cysts may play an important role in the survival and seasonal dynamics of *G. corollarium*. Whether the tiny and comparably fragile cysts are a part of the sexual reproduction cycle or whether they are produced asexually remains to be studied, but an ~5-month dormancy period has been confirmed for the *G. corollarium* cysts formed in culture (Parrow and Kremp 2008).

One of the most interesting findings of this study was the 100% sequence match of the D1-D2 domain of the LSU rDNA of the *G. corollarium* motile cell isolate (GCTV-B4) with isolates grown from a hitherto unidentified cyst type commonly found in sediment trap material from the open central and northern Baltic. The peculiar cyst, which has often preserved the typical dinoflagellate shape, can now be identified as *G. corollarium*. In contrast to the unspecific records of unidentified planktonic *Gymnodinium* species in the checklists, the numerous observations of the cysts in plankton and sediment trap samples within the HELCOM monitoring program can provide at least a rough picture of the distribution of *G. corollarium* in the Baltic Sea. Due to their characteristic shape, cysts have received special attention, and notes were made on their encounter. In the Swedish monitoring program, for example, the cysts were documented and referred to as *Gymnodinium* sp. ''*cosmarium-like,*'' due to its peculiar shape (S. Hajdu, personal observation). Because of their pronounced wall, they were sometimes also assigned to *Glenodinium* (R. Hansen, personal observation). Table 3 summarizes occurrence of the cysts in the Baltic Sea from monitoring records and presents associated cyst concentrations and cyst fluxes, respectively. This survey shows that *G. corollarium* may occur all through the Baltic Sea, from the Bornholm Sea (R. Hansen, personal observation) to the Bothnian Bay (S. Hajdu, personal observation).

Interestingly, cysts were often found in deeper water layers, probably reflecting sedimentation. Cyst fluxes, measured during May and early June by sediment traps in the Gotland Sea, approximately equal the sedimentation rates of *W. halophila* cysts at the southwest coast of Finland (Kremp and Heiskanen 1999). Standing stocks of the latter species associated with such sedimentation rates were on the order of 10^4 to 10^5 cells $\cdot L^{-1}$. It might be assumed that the reported concentrations of *G. corollarium* cysts correspond to similar abundances of motile cells in the water column. Together with the ecophysiological information, this finding clearly suggests that *G. corollarium* is a versatile species that is distributed throughout most of the Baltic Sea and is ecologically important for the Baltic ecosystem. To ascertain the distribution patterns of this species in time and space, and to gain more information on its ecology, there is a need for molecular identification techniques considering the identification problems associated with species within the genus *Gymnodinium* and the different, but morphologically similar, spring bloom dinoflagellates in the Baltic Sea.

Laboratory facilities were provided by the Tvärminne Zoological Station (University of Helsinki), the Department of Systems Ecology (Stockholm University), and the Phycology laboratory (University of Copenhagen). We thank Helena Höglander and Antonella Penna for discussion and Sanna Eirtovaara for assistance with the molecular work. Dr. Reijo

Pitkäranta (Department of Classical Languages, University of Helsinki) kindly translated the species diagnosis into Latin. This work was funded by the Walter and Andrée de Nottbeck Foundation (A. Sundström), SYNTHESYS (http://www.synthesys.info/), which is financed by European Community Research Infrastructure Action under the FP6 ''Structuring the European Research Area'' Programme (A. Sundström), and the Academy of Finland grant 111336 (A. Kremp).

Autio, R., Heiskanen, A.-S., Hällfors, G., Hällfors, S., Kaitala, S., Kivi, K., Kuosa, H., et al. 1990. *Ecological Plankton Research of the Baltic Sea-Project PELAG: Final Report 1987–89.* PELAG Press, Helsinki, Finland, 172 pp.

Biecheler, B. 1939. Sur deux Péridiniens nouveaux des eaux saumâtres des environs de Sète. *Bull. Soc. Zool. Fr.* 64:12–8.

Biecheler, B. 1952. Recherches sur les Péridiniens. *Bull. Biol. Fr. Belg.* 36(Suppl.):1–149.

Daugbjerg, N., Hansen, G., Larsen, J. & Moestrup, Ø. 2000. Phylogeny of some of the major genera of dinoflagellates based on ultrastructure and partial LSU rDNA sequence data, including the erection of three new genera of unarmoured dinoflagellates. *Phycologia* 39:302–17.

Daugbjerg, N., Moestrup, Ø. & Arctander, P. 1994. Phylogeny of the genus *Pyramimonas* (Prasinophyceae) inferred from the *rbc*L gene. *J. Phycol.* 30:991–9.

Dodge, J. D. & Crawford, R. M. 1969. The fine structure of *Gymnodinium fuscum* (Dinophyceae). *New Phytol.* 68:613–8.

Drebes, G. 1978. *Dissodinium pseudolunula* (Dinophyta), a parasite on copepod eggs. *Br. Phycol. J.* 13:319–27.

Ehrenberg, C. G. 1834. Dritter Beitrag zur Erkenntnis grosser Organisation in der Richtung des kleinsten Raumes – Abhandlungen der Königlichen Akademie der Wissenschaften zu Berlin. *Aus dem Jahre* 1833:145–336, pl. 1–11.

Ehrenberg, C. G. 1838. *Die Infusionsthierchen als vollkommene Organismen.* Voss, Berlin, 547 pp., pl. 1–64.

Elbrächter, M. & Drebes, G. 1978. Life cycles, phylogeny and taxonomy of *Dissodinium* and *Pyrocystis* (Dinophyta). *Helgol. Wiss. Meeresunters.* 31:347–66.

Fløe Jørgensen, M., Murray, S. & Daugbjerg, N. 2004. *Amphidinium* revisited. I. Redefinition of *Amphidinium* (Dinophyceae) based on cladistic and molecular phylogenetic analyses. *J. Phycol.* 40:351–65.

Guillard, R. R. L. & Lorenzen, C. J. 1972. Yellow-green algae with chlorophyllid *c*. *J. Phycol.* 8:10–4.

Guillard, R. R. L. & Ryther, J. H. 1962. Studies of marine planktonic diatoms. I. *Cyclotella nana* Hustedt and *Detonula confervacea* (Cleve) Gran. *Can. J. Microbiol.* 8:229–39.

Hajdu, S. 2002. Phytoplankton of Baltic environmental gradients: observations on potentially toxic species. PhD thesis, Department of Systems Ecology, Stockholm University, Stockholm, Sweden, 22 pp.

Hajdu, S. & Willén, T. 1985. *Development of Phytoplankton in the Gulf of Bothnia During May 1979–1984.* The Swedish Marine Association. Annual Report. SMHI Press, Norrköping, Sweden, pp. 161–71.

Hall, T. 2006. BioEdit: a user-friendly biological sequence alignment editor and analysis program for Windows 95/98/NT. *Nucleic Acids Symp. Ser.* 41:95–8.

Hällfors, G. 2004. Checklist of Baltic Sea phytoplankton species. *HELCOM, Balt. Sea Environ. Proc.* 95:1–210.

Hansen, G. 2001. Ultrastructure of *Gymnodinium aureolum* (Dinophyceae): toward a further redefinition of *Gymnodinium* sensu stricto. *J. Phycol.* 37:612–23.

Hansen, G., Botes, L. & de Salas, M. 2007. Ultrastructure and large subunit rDNA sequences of *Lepidodinium viride* reveal a close relationship to *Lepidodinium chlorophorum* comb. nov. (=*Gymnodinium chlorophorum*). *Phycol. Res.* 55:25–41.

Hansen, G., Daugbjerg, N. & Henriksen, P. 2000a. Comparative study of *Gymnodinium mikimotoi* and *Gymnodinium aureolum*, comb. nov. (=*Gyrodinium aureolum*) based on morphology, pigment composition, and molecular data. *J. Phycol.* 36:394–410.

Hansen, G., Moestrup, Ø. & Roberts, K. R. 2000b. Light and electron microscopial observations on the type species of *Gymnodinium*, *G. fuscum* (Dinophyceae). *Phycologia* 39:365–76.

Heiskanen, A.-S. 1993. Mass encystment and sinking of dinoflagellates during a spring bloom. *Mar. Biol.* 116:161–7.

HELCOM. 1990. Second periodic assessment of the state of the marine environment of the Baltic Sea, 1984–1988; background document. *Balt. Sea Environ. Proc.* 35B:1–432.

HELCOM. 1996. Third periodic assessment of the state of the marine environment of the Baltic Sea, 1989–1993; background document. *Balt. Sea Environ. Proc.* 64B:1–252.

Herdman, E. C. 1922. Notes on dinoflagellates and other organisms causing discolouration of the sand of Port Erin II. *Proc. Trans. Liverpool Biol. Soc.* 36:15–30.

Hobro, R. 1979. Stages of the annual phytoplankton succession in the Askö area (northern Baltic Sea). *Acta Bot. Fenn.* 110:79–80.

Höglander, H., Larsson, U. & Hajdu, S. 2004. Vertical distribution and settling of spring phytoplankton in the offshore NW Baltic Sea proper. *Mar. Ecol. Prog. Ser.* 283:15–27.

Hulburt, E. M. 1957. The taxonomy of unarmored Dinophyceae of shallow embayments of Cape Cod, Massachusetts. *Biol. Bull.* 112:196–219.

Jaanus, A., Hajdu, S., Kaitala, S., Andersson, A., Kaljurand, K., Ledaine, I., Lips, I. & Olenina, I. 2006. Distribution patterns of isomorphic cold-water dinoflagellates (*Scrippsiella/Woloszynskia* complex) causing 'red tides' in the Baltic Sea. *Hydrobiologia* 554:137–46.

Kofoid, C. A. & Sweezy, O. 1921. The free-living unarmoured dinoflagellata. *Mem. Univ. Calif.* 5:1–562.

Kononen, K. & Niemi, Å. 1984. Long term variation of the phytoplankton composition at the entrance to the Gulf of Finland. *Ophelia* 3(Suppl.):101–10.

Kremp, A., Elbrächter, M., Schweikert, M., Wolny, J. L. & Gottschling, M. 2005. *Woloszynskia halophila* (Biecheler) comb. nov.: a bloom-forming cold-water dinoflagellate co-occurring with *Scrippsiella hangoei* (Dinophyceae) in the Baltic Sea. *J. Phycol.* 41:629–42.

Kremp, A. & Heiskanen, A.-S. 1999. Sexuality and cyst formation of the spring bloom dinoflagellate *Scrippsiella hangoei* in the coastal northern Baltic Sea. *Mar. Biol.* 134:771–7.

Kuosa, H. 1986. The phytoplankton of a small brackish-water bay, Tvärminne Byviken, Southern Finland. *Ophelia* 4(Suppl.):119–27.

Larsen, J. 1994. Unarmoured dinoflagellates from Australian waters. 1. The genus *Gymnodinium* (Gymnodiniales, Dinophyceae). *Phycologia* 33:24–33.

Larsen, J., Kuosa, H., Ikävalko, J., Kivi, K. & Hällfors, S. 1995. A redescription of *Scrippsiella hangoei* (Schiller) comb. nov. – a 'red tide' forming dinoflagellate from the northern Baltic. *Phycologia* 34:135–44.

Lenaers, G., Maroteaux, L., Michot, B. & Herzog, M. 1989. Dinoflagellates in evolution. A molecular phylogenetic analysis of large subunit ribosomal RNA. *J. Mol. Evol.* 29:40–51.

Lignell, R., Heiskanen, A.-S., Kuosa, H., Gundersen, P., Kuuppo-Leinikki, R., Pajuniemi, R. & Uitto, A. 1993. Fate of a phytoplankton spring bloom: sedimentation and carbon flow in the planktonic food web in the northern Baltic. *Mar. Ecol. Prog. Ser.* 94:239–52.

Lilly, E. L., Halanych, K. M. & Anderson, D. M. 2005. Phylogeny, biogeography and species boundaries within the *Alexandrium minutum* group. *Harmful Algae* 4:1004–20.

Lindberg, K., Moestrup, Ø. & Daugbjerg, N. 2005. Studies on woloszynskioid dinoflagellates I: *Woloszynskia coronata* re-examined using light and electron microscopy and partial LSU rDNA sequences, with description of *Tovellia* gen. nov. and *Jadwigia* gen. nov (Tovelliaceae fam. nov.). *Phycologia* 44:416–40.

Moestrup, Ø., Lindberg, K. & Daugbjerg, N. 2009a. Studies on woloszynskioid dinoflagellates IV: the genus *Biecheleria* gen. nov. *Phycol. Res.* 57: in press.

Moestrup, Ø., Lindberg, K. & Daugbjerg, N. 2009b. Studies on woloszynskioid dinoflagellates V. Ultrastructure of *Biecheleriopsis*

gen. nov., with description of *B. adriatica* sp. nov. *Phycol. Res.* 57: in press.
Müller-Haeckel, A. 1985. Shade adapted algae beneath ice and snow in the Northern Bothnian Sea. *Int. Rev. Ges. Hydrobiol.* 70:325–34.
Murray, S. & Patterson, D. J. 2002. The benthic dinoflagellate genus *Amphidinium* in south-eastern Australian waters, including three new species. *Eur. J. Phycol.* 37:279–98.
Niemi, Å. 1975. Ecology of phytoplankton in the Tvärminne area, SW coast of Finland. II. Primary production and environmental conditions in the archipelago and the sea zone. *Acta Bot. Fenn.* 105:1–73.
Niemi, Å. 1986. Algsamhällen i havsisen. *Nordensk. Samfund. Tidskr.* 46:3–19.
Nunn, G. B., Theisen, B., Christensen, B. & Arctander, P. 1996. Simplicity-correlated size growth of the nuclear 28S ribosomal RNA D3 expansion segment in the crustacean order isopoda. *J. Mol. Evol.* 42:211–23.
Nygaard, G. 1949. Hydrobiological studies on some Danish ponds and lakes. Part II: the quotient hypothesis and some new or little known phytoplankton organisms. *Det. K. Dan. Vidensk. Selsk. Biol. Skr.* 7:1–293.
Olli, K., Heiskanen, A.-S. & Lohikari, K. 1998. Vertical migration of autotrophic planktonic microorganisms during a vernal bloom at the coastal Baltic Sea – coexistence through niche separation. *Hydrobiologia* 363:179–89.
Parrow, M. W. & Kremp, A. 2008. Asexual resting cysts: a common dinoflagellate survival strategy? In *Book of Abstracts Eighth International Conference on Modern and Fossil Dinoflagellates.* Unpublished, pp. 42–3.
Posada, D. & Crandall, K. A. 1998. Modeltest: testing the model of DNA substitution. *Bioinformatics* 14:817–8.
Rintala, J.-M., Spilling, K. & Blomster, J. 2007. Temporary cyst enables long-term dark survival of *Scrippsiella hangoei* (Dinophyceae). *Mar. Biol.* 152:57–62.
Ronquist, F. & Huelsenbeck, J. P. 2003. MRBAYES 3: Bayesian phylogenetic inference under mixed models. *Bioinformatics* 19:1572–4.
Schiller, J. 1932. Dinoflagellatae. *In* Kolkwitz, R. [Ed.] *Rabenhorst's Kryptogamenflora*, 10, Abt. 3, Teil I. Akademische Verlagsgesellschaft M. B. H, Leipzig, Germany, pp. 257–432.
Schilling, A. J. 1891. *Die Süsswasser-Peridineen.* Flora vol. 74. N. G. Elwert'sche Verlagsbuchhandlung, Marburg, Germany, pp. 220–99, taf viii–x.
Scholin, C. A., Herzog, M., Sogin, M. & Anderson, D. M. 1994. Identification of group-and strain-specific genetic markers for globally distributed *Alexandrium* (Dinophyceae). II. Sequence analysis of a fragment of the LSU rRNA gene. *J. Phycol.* 30:999–1011.
Skuja, H. 1956. Taxonomische und biologische Studien über das Phytoplankton Schwedischer Binnengewässer. *Nova Acta Reg. Soc. Sci. Upsaliensis. Ser. IV* 16:1–404.
Stein, F. [Ed.] 1883. *Der Organismus der Infusionsthiere.* 3. Abt. Der Organismus der Arthrodelen Flagellaten nach eigenen Forschungen in systematischer Reihenfolge bearbeitet. 2. Hälfte. Einleitung und Erklärung der Abbildungen. W. Engelmann, Leipzig, Germany, pp. 1–30, pl. 1–25.
Swift, E. 1973. *Dissodinium pseudolunula* n. sp. *Phycologia* 12:90–1.
Swofford, D. L. 2003. *PAUP* Phylogenetic Analysis Using Parsimony (*and Other Methods), Version 4.* Sinauer Associates, Sunderland, Massachusetts.
Tang, Y. Z., Egerton, T. A., Kong, L. & Marshall, H. G. 2008. Morphological variation and phylogenetic analysis of the dinoflagellate *Gymnodinium aureolum* from a tributary of Chesapeake Bay. *J. Eukaryot. Microbiol.* 55:91–9.
Thompson, J. D., Higgins, D. G. & Gibson, T. J. 1994. CLUSTAL W: improving the sensitivity of progressive multiple sequence alignment through sequence weighting, position specific gap penalties and weight matrix choice. *Nucleic Acids Res.* 22:4673–80.
Thomsen, H. A. 1992. *Plankton i de indre danske farvande. Havsforskning fra Miljøstyrelsen. Nr. 11.* Scantryk, Copenhagen, Denmark, 331 pp.
Wasmund, N., Nausch, G. & Matthäus, W. 1998. Phytoplankton spring bloom in the southern Baltic Sea – spatio-temporal development and long-term trends. *J. Plankton Res.* 20:1099–117.
Wasmund, N. & Uhlig, S. 2003. Phytoplankton trends in the Baltic Sea. *ICES J. Mar. Sci.* 60:177–86.
Wedemayer, G. J., Wilcox, L. W. & Graham, L. E. 1982. *Amphidinium cryophilum* sp. nov. (Dinophyceae) a new freshwater dinoflagellate. I. Species description using light and scanning electron microscopy. *J. Phycol.* 18:13–7.
Wilcox, L. W. & Wedemayer, G. J. 1984. *Gymnodinium acidotum* Nygaard (Pyrrophyta), a dinoflagellate with an endosymbiotic cryptomonad. *J. Phycol.* 20:236–42.
Wilcox, L. W., Wedemayer, G. J. & Graham, L. E. 1982. *Amphidinium cryophilum* sp. nov. (Dinophyceae) a new freshwater dinoflagellate. II. Ultrastructure. *J. Phycol.* 18:18–30.

Supplementary Material

The following supplementary material is available for this article:

Table S1. Alphabetical list of species included in the phylogenetic analyses. Strain numbers and GenBank accession numbers are also provided.

This material is available as part of the online article.

Please note: Wiley-Blackwell are not responsible for the content or functionality of any supplementary materials supplied by the authors. Any queries (other than missing material) should be directed to the corresponding author for the article.